

Entropy production in the cyclic lattice Lotka-Volterra model

Celia Anteneodo

Centro Brasileiro de Pesquisas Físicas,
Rua Dr. Xavier Sigaud 150, 22290-180, Rio de Janeiro, RJ, Brazil.

The cyclic Lotka-Volterra model in a D -dimensional regular lattice is considered. Its “nucleus growth” mode is analyzed under the scope of Tsallis’ entropies $S_q = (1 - \sum_i p_i^q)/(q-1)$, $q \in \mathbb{R}$. It is shown both numerically and by means of analytical considerations that a linear increase of entropy with time, meaning finite asymptotic entropy rate, is achieved for the entropic index $q_c = 1 - 1/D$. Although the lattice exhibits fractal patterns along its evolution, the characteristic value of q can be interpreted in terms of very simple features of the dynamics.

I. INTRODUCTION

Over a decade ago, Tsallis proposed an entropic form as a starting point for a possible generalization of Boltzmann-Gibbs statistics [1] (see also [2] for a review on the subject). The generalized entropy has the form

$$S_q = k \frac{1 - \int dx [\rho(x)]^q}{q-1}, \quad \text{with } q \in \mathbb{R}, \quad (1)$$

where k is a positive constant and ρ a normalized probability density. The usual Boltzmann-Gibbs-Shannon (BGS) entropy is recovered when $q = 1$ [$S_1 = -k \int dx \rho(x) \ln \rho(x)$].

Many experimental and numerical data are well approximated by q -exponentials (the probability distributions that maximize S_q under simple constraints), giving support to the applicability of the new entropic measure to those systems. In the case of the high-dimensional systems of interest in statistical physics, first-principle derivations are still to be made. However, Tsallis’ entropy seems to be the appropriate one for certain low-dimensional dynamical systems, such as unimodal maps at the edge of chaos, where the usual Lyapunov exponent vanishes. In such cases the characteristic value of q is related to relevant properties of the dynamics and it can be calculated by several paths, such as the multifractal spectrum of the attractor [3] or the sensitivity to initial conditions [4], or even, from a rigorous renormalization group analysis [5]. Furthermore, this scenario has been shown to be valid also for two-dimensional maps [6].

One of the properties of S_q that, for an appropriate value of the entropic index, can make it in some cases preferable to the standard entropy is the possibility of having an asymptotic rate of entropy production with a non-trivial value. Among the *a priori* infinite possible values of q , the one leading to a linear increase of the entropy with time, implying *finite* rate of entropy growth, is selected as being q_c , a value of q characteristic of the system. In fact, this is another path for the determination of q that in the case of unimodal maps provides the same

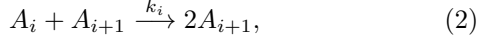
results [7] as the alternative methods mentioned above. Moreover, rigorous analytical results have recently been found for such systems along this line [8]. The temporal evolution of the S_q family, allowing to determine q_c , has also been investigated for diverse other dynamical systems [9–12]. The outcome $q_c \neq 1$ has usually been interpreted as a signal of nonextensivity.

Under the scope of the generalized entropies S_q , we will study in the present paper the temporal evolution of a cyclic Lotka-Volterra model in the lattice (LLV) [13,14]. This model is particularly rich as it exhibits interesting features, such as stationary states with spatial patterns [13] and fractality [15], which makes it a potential candidate for the applicability of the entropies S_q . The LLV is one of the descendants of the original versions constructed by Lotka [16] and Volterra [17] to model autocatalytic chemical reactions and the prey-predator dynamics, respectively, and further adapted to many other situations from active transport by proteins [18] to social processes [19]. The generalized LLV extends the original scheme to \mathcal{N} species A_i ($i = 1, \dots, \mathcal{N}$) such that, cyclically, A_i is “predator” of A_{i-1} and simultaneously “prey” of A_{i+1} (with $A_{\mathcal{N}+1} \equiv A_1$). Furthermore, the dynamics takes place over a lattice, an ingredient that introduces new interesting spatial features in comparison to the spatially homogeneous mean-field description [20].

The criterion of finite entropy rate has been applied before to the LLV model in one and two dimensions [12] and the relation $q_c = 1 - 1/D$ was conjectured for arbitrary D . Now we will extend that study to higher dimensions in order to test the conjecture. Moreover, we will essay an interpretation of the connection between q_c and space dimensionality, showing that $q_c \neq 1$ is not necessarily related to the fractal properties of the dynamics. The remaining of the paper is organized as follows. In Sect. II we describe in detail the specific LLV model considered. In Sect. III the time behavior of the entropies S_q associated to the LLV is studied. Sect. IV exhibits the behavior of S_q under simple transformations of a probability density leading to reanalyze in Sect. V the LLV dynamics. Final remarks are presented in Sect. VI.

II. THE GENERALIZED LOTKA-VOLTERRA MODEL IN A LATTICE

Particles of the \mathcal{N} different species A_i are localized at the sites of a D -dimensional hypercubic lattice. Reactions between particles of different species occur in bimolecular autocatalytic steps following the scheme



for $i = 1, \dots, \mathcal{N}$, being $A_{\mathcal{N}+1} \equiv A_1$, and where $0 \leq k_i \leq 1$ are the kinetic rates. No sites are empty but one of the species could be interpreted as representing empty sites in the lattice [12,14,15,21]. The dynamics is implemented by means of a Monte Carlo (MC) algorithm following the details in Refs. [12,14,15]. Basically, at every microscopic step: (i) one lattice site is randomly chosen; (ii) one of its nearest neighbors is randomly chosen; (iii) if the first site is A_i and the neighbor A_{i+1} , the first site changes to A_{i+1} with probability k_i , in accord with scheme (2), otherwise the site remains unchanged. Each MC step (MCS, our unit of time) consists in $N = L^D$ microscopic steps defined above, where L is the linear size of the lattice, so that at each MCS all sites are revisited once in average. Boundary conditions are periodic. In this paper we will deal with three species only ($\mathcal{N} = 3$) and we will focus on the symmetric case where all the kinetic rates are equal to one ($k_1 = k_2 = k_3 = 1$). Moreover, we will restrict our study to a particular mode of the dynamics, the “nucleus growth” one [12,21]. The lattice is set with all the sites filled with species A_3 and a “droplet” or nucleus represented by a sublattice of small linear size λ (i.e., $\lambda \ll L$) is introduced. The droplet contains equal amounts of particles of all the three species randomly and uniformly distributed.

As the system evolves according to the MC dynamics, the droplet grows and acquires spontaneously a peculiar structure [22]. Typical snapshots of the dynamics are exhibited in Fig. 1 for lattices in $D = 2, 3$ and 4 dimensions. Rings of alternating species develop, repeating the sequence A_1, A_2, A_3 towards the center of the droplet. This pattern is possible since all the kinetic constants are equal, then layers have almost the same radial velocity. The thickness of the rings decreases towards the center and thickness fluctuations destroy the most immersed rings. This behavior has already been observed before by Provata and Tsekouras for the two dimensional case [21]. They also observed that the destroyed rings give rise to a spatial organization of the species in domains with fractal boundaries typical of the steady state in fully occupied periodical lattices [12,15,21]. As the dimensionality increases, spatial features remain qualitatively similar but length scales become shorter. In the mean-field limit $D \rightarrow \infty$, homogeneity is expected. We are going to inspect immediately the evolution of spatial patterns from the viewpoint of the generalized entropies S_q .

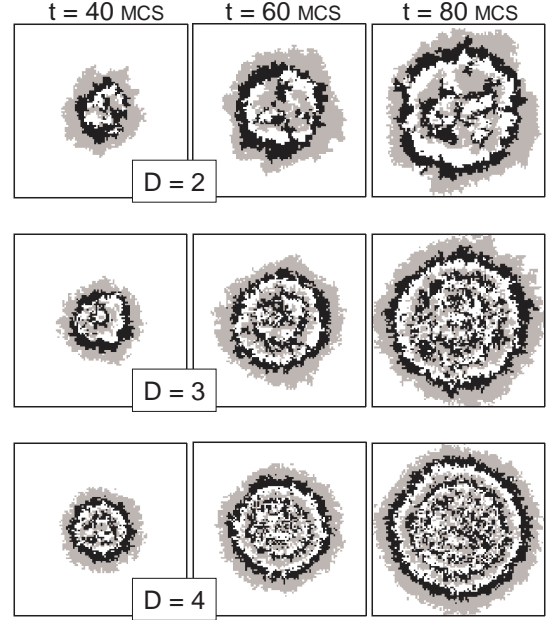


FIG. 1. Snapshots of the dynamics at different times indicated on the top of the figure, for $D = 2, 3$ and 4. The initial condition is a droplet, where all the species are present in equal amounts and homogeneously distributed, over a background of A_3 . In all cases the linear size of the lattice is $L = 100$ and the initial nucleus has $\lambda = 6$. For $D > 2$ the snapshots correspond to sections parallel to one of the hypercube faces and passing by the position of the center of the initial droplet. Species are A_1 (gray), A_2 (black) and A_3 (white).

III. TEMPORAL EVOLUTION OF S_q IN THE LLV

Following previous work [12], we study the temporal evolution of the entropies associated to one of the species, e.g., A_1 . This particular choice does not substantially affect the results. Nonoverlapping windows or sublattices $\{W_i, 1 \leq i \leq M\}$ of edge length l covering all the lattice are considered. Thus the number of windows must be $M = (L/l)^D$, where l is a divisor of L . We associate to each window i a probability $p_i(t)$ of being occupied by species A_1 at time t by counting the number of particles of that species $n_1(i, t)$. Then $p_i(t) = n_1(i, t)/n_1(t)$, where $n_1(t)$ is the total number of particles A_1 on the lattice. The resulting set of probabilities is used to calculate the entropy of the lattice, given by the discrete version of Eq. (1) (where we have set $k = 1$)

$$S_q = \frac{1 - \sum_i p_i^q}{q - 1}. \quad (3)$$

The LLV in $D = 1$ and 2 dimensions has already been studied from this viewpoint before [12]. Now we will investigate higher dimensional lattices. Fig. 2 shows

the generalized entropies as a function of time for diverse values of q , when the lattice has $D = 3$ and 4 dimensions. The results shown in Fig. 2 are not qualitatively affected by changing l and L , as long as $1 \leq l \ll L$. They mainly affect the saturation level, $S_q^{sat.} = [(L/l)^{D(1-q)} - 1]/(1-q)$ for a uniform distribution.

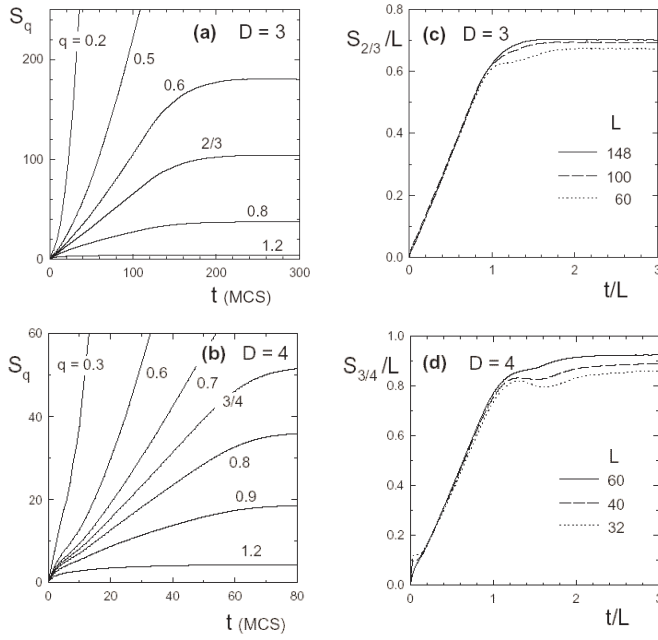


FIG. 2. Time evolution of the generalized entropies. S_q vs. t for various values of q and $L = 148$ in $D = 3$ (a), $L = 60$ in $D = 4$ (b). S_q/L vs. t/L for different lattice sizes L with: $q = 2/3$ when $D = 3$ (c), $q = 3/4$ when $D = 4$ (d). Symbols correspond to a single representative numerical experiment. In all cases, the window of the partitioning is $l = 4$ and the initial droplet size $\lambda = 4$.

Notice in Figs. 2.a and 2.b that as q increases the concavity passes from positive to negative, before saturation, which occurs when the droplet radius becomes of the order of the linear size of the lattice. Entropies with q yielding constant slope (null concavity) are represented as a function of time in Figs. 2.c and 2.d. In all cases, constant slope occurs at a value of the entropic index q_c that as function of D follows the law

$$q_c \simeq 1 - \frac{1}{D}, \quad (4)$$

in agreement with the relation numerically found for $D = 1$ and 2, and conjectured for generic D previously [12]. See Fig. 3.

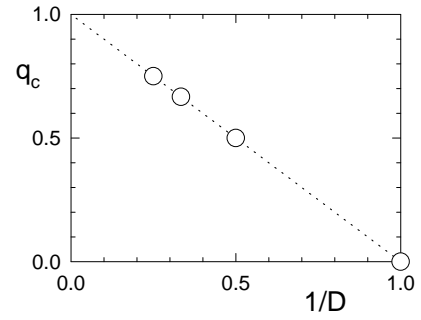


FIG. 3. Characteristic value q_c as a function of the lattice dimensionality D . The dotted straight line corresponds to $q_c = 1 - 1/D$. Symbols are the result of numerical experiments. Errors are of the order of symbol size. For $D = 3$ and 4: q_c was numerically determined from the data in Fig. 2 as the value of q yielding a linear slope. For $D = 1$ and 2, q_c was extracted from Ref. [12].

IV. BEHAVIOR OF S_q UNDER SIMPLE TRANSFORMATIONS OF A PROBABILITY DENSITY

The characteristic entropic index q_c is related to the number of dimensions D through a simple law. This leads to think that a simple mechanism could be behind. Since we are dealing with a growth process, we will investigate in this Section the relation between q_c and D resulting from some basic growth mechanisms and connect it with Eq. (4).

Let us analyze the behavior of the entropies S_q under a rescaling transformation of an arbitrary probability density $\rho(x)$, being x a point in a D -dimensional space [23]. The entropy of the rescaled function $\rho_\sigma(x) = \rho(x/\sigma)/\sigma^D$, where σ is a linear length, becomes

$$S_q(\sigma) = \frac{\sigma^{(1-q)D} \left((1-q)S_q(1) + 1 \right) - 1}{1-q}. \quad (5)$$

As $\sigma \rightarrow \infty$, the distribution broadens and the entropy grows due to the loss of order. If the scaling or stretching parameter increases exponentially with time, linear entropy increase occurs for $q = 1$. If the scaling parameter follows the law $\sigma \sim t^{\gamma/2}$ with $\gamma > 0$, then the generalized entropies increase with time as follows: For $q < 1$, they scale with time as $S_q(t) \sim t^{(1-q)D\gamma/2}$, $S_q(t) \sim \ln t$ in the marginal case $q = 1$, and for $q > 1$, saturation occurs at $S_q(\infty) = 1/(q-1)$. Hence a linear increase is achieved in the regime $q < 1$ for

$$q_c = 1 - \frac{2}{\gamma D}. \quad (6)$$

As a relevant particular case let us mention the normal diffusive spreading of a D -dimensional Gaussian distribution where the stretching parameter is $\sigma^2(t) = 2Qt$, with Q the positive diffusion constant. In this case $\gamma = 1$ then

$q_c = 1 - 2/D$. The general case given by Eq. (6) may be due to anomalous diffusive motion. A still simpler example of rescaling transformation that will be useful later consists in a density being non-null and uniform inside a D -dimensional hypersphere and zero outside, such that the radius $\sigma(t)$ grows as $\sigma \sim t^{\gamma/2}$. Notice that the expression for q_c of the growing LLV droplet, given by Eq. (4), is obtained when the temporal variation of the scaling length σ is ballistic ($\gamma = 2$).

Now, let us consider another simple process. $M \gg N$ windows cover a lattice, like for the LLV in the previous Section, with probabilities

$$(p_1, p_2, \dots, p_N, \underbrace{0, 0, \dots, 0}_{M-N}), \quad \sum_{1 \leq i \leq N} p_i = 1.$$

Imagine that windows with non-null probability are replicated by an integer factor m such that the new set of probabilities is

$$\underbrace{\left(\frac{p_1}{m}, \dots, \frac{p_1}{m}, \frac{p_2}{m}, \dots, \frac{p_2}{m}, \dots, \frac{p_N}{m}, \dots, \frac{p_N}{m}\right)}_m, \underbrace{\left(\frac{p_1}{m}, \dots, \frac{p_1}{m}, \frac{p_2}{m}, \dots, \frac{p_2}{m}, \dots, \frac{p_N}{m}, \dots, \frac{p_N}{m}\right)}_m, \dots, \underbrace{\left(\frac{p_N}{m}, \dots, \frac{p_N}{m}, 0, 0, \dots, 0\right)}_{M-mN}$$

If the replication factor is $m \sim \sigma^D$ (where σ is a typical linear size of the D -dimensional system) and additionally if $\sigma \sim t^{\gamma/2}$, then the entropy will be produced in such a way that a growth linear in time occurs for q_c given by Eq. (6). In fact, if a continuous distribution is discretized, the associated rescaling process can be thought as a particular case of the replication one here considered, a special case where replicas are spatially ordered. Nevertheless for discrete probabilities, the entropic form S_q does not depend on the spatial localization of the windows.

Summarizing, while for an ordinary exponential growth process, the standard entropy S_1 increases linearly with t ; for a process where growth follows a power-law in time, S_q has the property of finite asymptotic entropy rate for some $q = q_c \neq 1$. This value of the entropic index can result from simple transformations and therefore may be trivially related to the lattice dimensionality. These ideas lead us to review the results of the precedent Section to see whether simple mechanisms are also lurking there.

V. SOME DETAILS OF THE LLV DYNAMICS

Let us inspect first the roughness of the interface because the reaction rate and therefore the dynamics of the propagating front are related to that quantity. Since we are interested in the interface, one can perform numerical simulations considering just two species. Hence we follow the evolution of an initial nucleus containing only A_1 particles dropped over a background of A_3 . Its propagation is like in the LLV case where a forefront of A_1 particles governs the spreading of the droplet. Since the reaction rate must be proportional to the “extent” of the

interface, we measure N_s , the number of reactive sites constituting the interface, and N_f , the total number of reactive faces in interfacial sites. Reactive faces are those separating two nearest neighboring sites occupied by different species. A suitable quantity for our model is

$$r = \frac{N_f}{cN_s}, \quad (7)$$

where c is the connectivity, i.e., the number of first nearest neighbors *per* site ($c = 2D$ in hypercubic lattices). The quantity r represents an averaged measure of the degree of reactivity of an interfacial site, and must be also connected to the roughness of the interface. The reactivity r is plotted in Fig. 4.a as a function of time. It soon reaches a stationary value within small fluctuations. For comparison, the figure also exhibits the value of r for a regularly filled hypersphere with the same total number of cells as in the LLV nucleus at each given t . The higher the lattice dimensionality, the larger the relative difference between the values of r for the two models. The roughness of the propagation front in the 1D dynamics has been studied in detail by Provata and Tsekouras [21]. Also in this case, it was shown that after a brief transient the rough profile remains stable in average.

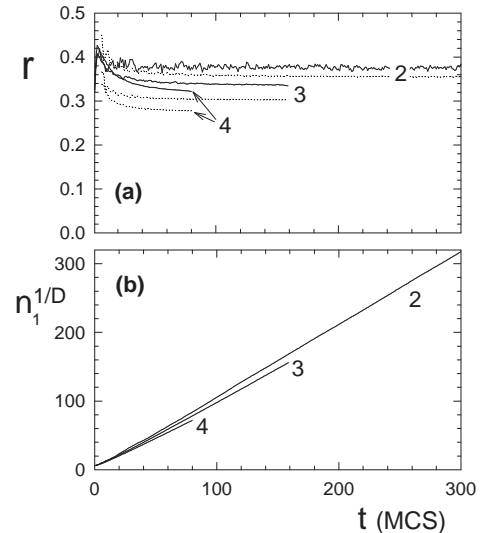


FIG. 4. Propagation of a droplet of A_1 in a lattice filled with A_3 , for different values of D indicated in the figure. (a) Reactivity r as a function of time for the two-species LLV (full lines); for comparison, r for a regularly filled hypersphere with the same total number of cells as the corresponding LLV nucleus is also plotted (dotted lines). (b) Total number of sites n_1 occupied by A_1 vs. time. The initial nucleus has linear size $\lambda = 4$.

If the reactivity remains constant in time, the front moves at constant radial speed: $R(t) = R(0) + vt$, where R is an effective radius $R \propto n_1^{1/D}$ and the velocity $v \equiv v(r)$ an increasing function of its argument for a

given D . Although the fractal properties of the interface are embodied in the velocity, if the roughness soon reaches its steady value, then fractality does not affect the temporal law of the front propagation. In effect, the linear dependence of R with time is observed in numerical experiments (see Fig. 4.b). Therefore, following the considerations of the precedent Section, Eq. (6) with $\gamma = 2$ must clearly hold in this binary case.

In the three-species case, although the reaction scheme is cyclic, symmetry is broken by the initial condition. Species A_3 plays the special role of a background what in turn makes A_1 play the special role of the forefront species. After a short transient and before the limits of the lattice are reached by the nucleus, the stationarity of the interface reactivity r , leads to a linear growth of the effective radius with time, as in the two species case. Consequently, the total number of cells in the nucleus, protected by the most external ring constituted by A_1 cells, will increase as t^D . Behind the first ring, the three species are equivalent, then the total number of cells occupied by each species in the nucleus is expected to increase with the same law t^D too. In fact, this behavior is observed in numerical simulations, as shown in Fig. 5, although species A_1 yields a slightly larger slope than A_2 . Linear growth implies a regime where the concentrations in the nucleus are conserved. When full occupation of the lattice is attained, the concentration of each species $c_i = n_i/L^D$ ($i = 1, \dots, 3$) fluctuates around the stable center predicted by the mean-field theory: $c_i = k_i/\sum_j k_j = 1/3$, for all i [14].

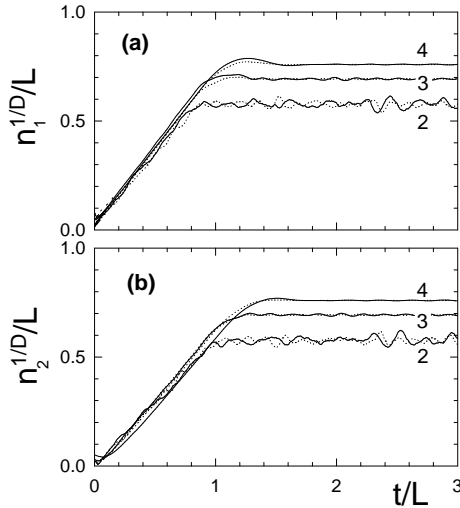


FIG. 5. Time evolution of the number of cells n_1 and n_2 occupied by species A_1 (a) and A_2 (b), respectively, for the values of the lattice dimensionality indicated in the figure and for various lattice sizes L : 150 and 200 ($D = 2$), 100 and 150 ($D = 3$), and 60 and 100 ($D = 4$), represented by dotted and full lines respectively. Time is measured in MCS. Curves correspond to single runs. The initial droplet size is $\lambda = 6$ for $D = 2$ and $\lambda = 4$ for $D = 3, 4$.

We have seen that the production of the species in the nucleus is such that after a short transient their concentrations remain approximately constant. Thus, in the extreme case when windows have the size of a cell ($l = 1$), a linear increase of S_q with time occurs clearly for q given by Eq. (4). In fact there will be n_1 windows with non-null probability $1/n_1$, where $n_1(t) \sim t^D$, then $S_q(t) = (n_1^{1-q} - 1)/(1 - q)$, so that: $S_q \sim t$, if $(1 - q)D = 1$. In the opposite extreme where windows are so large that all non-empty windows have approximately the same occupation number, that same temporal dependence is obtained too.

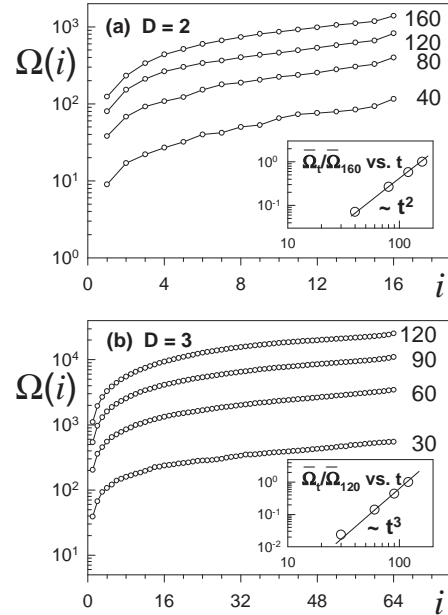


FIG. 6. Cumulative distribution of occupation numbers at different times (in MCS) indicated in the figure for $D = 2$ (a) and $D = 3$ (b). $\Omega(i)$ is the number of windows occupied by less than i cells of species A_1 ($1 \leq i \leq l^D$). In all cases, the window edges have length $l = 4$. For $D = 2$, $(L, \lambda) = (200, 6)$, and for $D = 3$, $(L, \lambda) = (148, 4)$. Insets: multiplication factor $\bar{\Omega}_t/\bar{\Omega}_{t_{max}}$ as a function of time (in MCS), where the horizontal bars mean average over all the occupation numbers at a given t , and $t_{max} = 160$ (a), 120 (b).

Let us analyze what happens for intermediate window sizes. Clusters of cells of each species like in fully occupied lattices [12,15] appear in the interior of the nucleus. It is not counterintuitive the idea that as the volume of the nucleus is increasing, the size distribution of the agglomerates becomes stationary after a transient. To test this idea one can calculate for instance the occupation numbers of the windows, intimately related to entropy computation, and see how their distribution evolves in time. Fig. 6 exhibits the number of windows $\Omega(i)$ occupied by at most i cells of species A_1 ($1 \leq i \leq l^D$), for different time instants. The occupation number for $i = 0$ is dismissed whereas it does not contribute to the entropy and a cumulative probability is considered in order to get

smoother curves. Notice that the curves in the log-linear plot are practically parallel, indicating that they differ in a multiplicative factor. Moreover, the replication factor increases following the law t^D as illustrated in the inset of Fig. 6 and in accord with previous considerations. All this means that a replication of the windows as described in Sect. IV with $\gamma = 2$ is going on.

In conclusion, although the underlying dynamics is complex, once the properties of spatial structures attain steady values, growth is controlled by simple laws. More specifically, the resulting growth processes are power-law in time with scaling exponents trivially related to the lattice dimensionality (with $\sigma \sim t$ or, equivalently, $\gamma = 2$). Then, the linear increase of S_q with time for q_c given by Eq. (4) is expected.

VI. FINAL REMARKS

In this paper we employed the criterion of finite asymptotic growth rate of S_q to determine q_c in the D -dimensional LLV. We verified for $D = 3$ and $D = 4$ a conjecture for the connection between q_c and D previously proposed [12], namely, $q_c = 1 - 1/D$. Moreover we exhibited the mechanisms leading to such relation.

The box-counting method applied to the 2D LLV [15] has shown that the boundaries of the small domains of a given species are approximately fractal [15] with a fractal dimension d_f that depends on the reaction rates k_i . Analogous results are expected in higher dimensions. We have seen that, for the present model and for the particular probability assignment considered, S_q entropy production does not capture directly the fractality of spatial patterns. Of course, since the fractal dimension d_f must depend on the lattice spatial dimension D , the characteristic entropic index q_c (a function of D) results in some way connected to d_f . But q_c is not determined by the degree of fractality, it is only determined by D , independently of the nature (fractal or not) of the growing core. This is so because the properties of spatial patterns, such as the interface roughness, soon reach steady values.

In a process where the number of occupied cells increases exponentially with time t , the usual BGS entropy S_1 increases linearly with t . For a growth process that is not exponential, one can not expect a linear increase of the standard entropy S_1 . If growth occurs following a power-law in time, S_q has the property of finite production rate for some $q = q_c \neq 1$. Then $q_c \neq 1$ is the expected behavior in these cases and it is not necessarily connected to the complex features of a system. So q_c may result trivially related to the lattice dimensionality.

We have shown that the stationarity of certain properties of the LLV dynamics determines a growth process linear in time ($\gamma = 2$), yielding relation (4). Although simple, this relation is in some way a consequence of the complex LLV dynamics. As perspectives, one can not exclude the possibility that in other dynamical regimes

of the LLV, the increase of S_q can reflect complex features directly. Also, it could be insightful to review previous works in the literature by taking into consideration the present results. This might be especially fruitful in cases where characteristic indexes of the form $q_c = 1 - 2/(\gamma D)$ have also been found, as in the interesting study of Galilean-invariant lattice Boltzmann models of fluids [11].

ACKNOWLEDGMENTS:

I am very grateful to Fulvio Baldovin and Constantino Tsallis for interesting and fruitful discussions. I also thank Astero Provata for useful comments on the LLV. This work was supported by Brazilian agencies FAPERJ and PRONEX.

-
- [1] C. Tsallis, J. Stat. Phys. **52**, 479 (1988).
 - [2] *Nonextensive Statistical Mechanics and Thermodynamics*, edited by S. R. A. Salinas and C. Tsallis, Braz. J. Phys. **29** 1999; *Nonextensive Statistical Mechanics and its Applications*, edited by S. Abe and Y. Okamoto, Lecture Notes in Physics Vol. 560 (Springer-Verlag, Heidelberg, 2001); *Non-Extensive Thermodynamics and Physical Applications*, edited by G. Kaniadakis, M. Lissia, and A. Rapisarda [Physica A **305** (2002)]; *Anomalous Distributions, Nonlinear Dynamics and Nonextensivity*, edited by H. L. Swinney and C. Tsallis [Physica D (2004)], in press. *Nonextensive Entropy - Interdisciplinary Applications*, edited by M. Gell-Mann and C. Tsallis (Oxford University Press, New York, 2004).
 - [3] M.L. Lyra and C. Tsallis, Phys. Rev. Lett. **80**, 53 (1998).
 - [4] C. Tsallis, A.R. Plastino and W.-M. Zheng, Chaos Solitons Fractals **8**, 885 (1997); U.M.S. Costa, M.L. Lyra, A.R. Plastino and C. Tsallis, Phys. Rev. E **56**, 245 (1997).
 - [5] F. Baldovin and A. Robledo, Phys. Rev. E **66**, 045104 (2002); Europhys. Lett. **60**, 518 (2002).
 - [6] U. Tirnakli, Phys. Rev. E **66**, 066212 (2002).
 - [7] V. Latora, M. Baranger, A. Rapisarda and C. Tsallis, Phys. Lett. A **273** 97 (2000); M. Baranger, V. Latora and A. Rapisarda, Chaos, Solitons and Fractals **13** 471 (2002).
 - [8] F. Baldovin and A. Robledo, cond-mat/0304410.
 - [9] U. Tirnakli, G.F.J. Ananos and C. Tsallis, Phys. Lett. A **289**, 51 (2001).
 - [10] N. Lemke and R.M.C. de Almeida, Physica A **325**, 396 (2003).
 - [11] B.M. Boghosian, P.J. Love, P.V. Coveney, I.V. Karlin, S. Succi and J. Yepez, Phys. Rev. E **68** 025103 (2003).
 - [12] G.A. Tsekouras, A. Provata and C. Tsallis, Phys. Rev. E **69**, 016120 (2004).
 - [13] K.-I. Tainaka, Phys. Rev. Lett. **63**, 2688 (1989).

- [14] A. Provata, G. Nicolis and F. Baras, J. Chem. Phys. **110**, 8361 (1999).
- [15] G.A. Tsekouras and A. Provata, Phys. Rev. E **65**, 016204 (2002).
- [16] A.J. Lotka, Proc. Natl. Acad. Sci. U.S.A. **6**, 410 (1920).
- [17] V. Volterra, *Leçons sur la théorie mathématique de la lutte pour la vie* (Gauthier-Villars, Paris, 1931).
- [18] F.M.C. Vieira and P.M. Bisch, Physica A **199**, 40 (1993).
- [19] J.M. Epstein, *Nonlinear dynamics, mathematical biology, and social science* (Addison-Wesley, Don Mills-Ontario, 1997).
- [20] L. Frachebourg, P. L. Krapivsky and E. Ben-Naim, Phys. Rev. E **54**, 6186 (1996).
- [21] A. Provata and G.A. Tsekouras, Phys. Rev. E **67**, 056602 (2003).
- [22] Occasionally, if the initial droplet is too small, it may be invaded by one of the species.
- [23] C. Anteneodo and A.R. Plastino, Phys. Lett. A **223**, 348 (1996).